

Macroscopic stiffening of embryonic tissues via microtubules, RhoGEF and the assembly of contractile bundles of actomyosin

Jian Zhou^{1,*†}, Hye Young Kim^{1,*}, James H.-C. Wang² and Lance A. Davidson^{3,‡}

SUMMARY

During morphogenesis, forces generated by cells are coordinated and channeled by the viscoelastic properties of the embryo. Microtubules and F-actin are considered to be two of the most important structural elements within living cells accounting for both force production and mechanical stiffness. In this paper, we investigate the contribution of microtubules to the stiffness of converging and extending dorsal tissues in *Xenopus laevis* embryos using cell biological, biophysical and embryological techniques. Surprisingly, we discovered that depolymerizing microtubules stiffens embryonic tissues by three- to fourfold. We attribute tissue stiffening to Xlfc, a previously identified RhoGEF, which binds microtubules and regulates the actomyosin cytoskeleton. Combining drug treatments and Xlfc activation and knockdown lead us to the conclusion that mechanical properties of tissues such as viscoelasticity can be regulated through RhoGTPase pathways and rule out a direct contribution of microtubules to tissue stiffness in the frog embryo. We can rescue nocodazole-induced stiffening with drugs that reduce actomyosin contractility and can partially rescue morphogenetic defects that affect stiffened embryos. We support these conclusions with a multi-scale analysis of cytoskeletal dynamics, tissue-scale traction and measurements of tissue stiffness to separate the role of microtubules from RhoGEF activation. These findings suggest a re-evaluation of the effects of nocodazole and increased focus on the role of Rho family GTPases as regulators of the mechanical properties of cells and their mechanical interactions with surrounding tissues.

KEY WORDS: Morphogenesis, Cell traction, Force production, Cellular mechanics, *Xenopus*

INTRODUCTION

The basic body plan of the vertebrate embryo is sculpted by tissue movements during morphogenesis and organogenesis. Such sculpting requires the application of forces by cells and tissues in the embryo against stiff mechanical structures in the early embryo. Forces must deform cells and their neighbors locally, and these forces are transmitted across many cells to deform surrounding embryonic tissues. Morphogenetic movements then depend on both the pattern of force generation, and on the spatial distribution of viscoelastic resistance. For example, medial-lateral intercalation of cells will drive convergence and extension only if the forces generated are sufficient to deform the surrounding tissue, and the converging cells are stiff enough not to absorb all of the deformation themselves. Force generation must exceed mechanical resistance, and force generation and resistance together dictate the speed and direction of tissue movements. Ultimately, molecular genetic processes control both force production and regulation of tissue stiffness within the embryo but little is known quantitatively about how these mechanical processes function together. Observations of cell movements or cell shape changes thus reveal

only part of the physical mechanisms that drive embryonic development and do not directly reveal the physical mechanical context of tissue movements.

Recent studies have revealed how mechanical properties are regulated within tissues (Zhou et al., 2009) and suggest how mechanical properties can alter the course of cell differentiation and morphogenesis (Wozniak and Chen, 2009). More generally, one of the central aims of developmental biologists has been to quantitatively describe macroscopic tissue movements, cell movements and coordinated cell shape changes (Stern, 2004; Trinkaus, 1984). For example, molecular polarity cues such as chemotactic gradients can drive migration. Large-scale coordinated cell rearrangement during gastrulation is regulated by the planar cell polarity (PCP) pathway. Cell or tissue response to chemotactic signals or activation of the PCP pathway depends both on specific details of the molecular programs, as well as on the mechanical context in which they play out (Davidson et al., 2009). One of the more complex aspects of morphogenesis is that proteins such as myosin II contribute to force generation as well as to cell and tissue mechanical properties such as stiffness (Zhou et al., 2009).

Microtubules and F-actin are considered to be two of the most important structural elements within living cells accounting for both force production (Chan and Odde, 2008; Cojoc et al., 2007) and their mechanical stiffness (Janmey, 1991; Janmey et al., 1991; Valentine et al., 2005). However, the precise role of microtubules in establishing the mechanical properties of cells and tissues is still not clear. For example, reduction of microtubule network can leave cell stiffness unchanged (Collinsworth et al., 2002; Rotsch and Radmacher, 2000; Takai et al., 2005; Trickey et al., 2004), reduced (Nagayama and Matsumoto, 2008; Potard et al., 1997; Sato et al., 1990; Wang, 1998) or increased (Stamenovic et al., 2002a; Wu et

¹Department of Bioengineering, Biomedical Science Tower 3-5059, 3051 Fifth Avenue, University of Pittsburgh, Pittsburgh, PA 15261, USA. ²Departments of Orthopedic Surgery and Bioengineering, University of Pittsburgh, Pittsburgh, PA 15213, USA. ³Department of Bioengineering and Developmental Biology, University of Pittsburgh, Pittsburgh, PA 15213, USA.

*These authors contributed equally to this work

[†]Present address: 2121 Engineering Hall, University of California, Irvine, CA 92697, USA

[‡]Author for correspondence (lad43@pitt.edu)

al., 2000). Disruption of microtubules can also increase cellular tension (Danowski, 1989; Dennerll et al., 1988; Kolodney and Elson, 1995; Stamenovic et al., 2002b; Wang et al., 2001) by activating actomyosin contraction; but it is unknown whether activation of actomyosin in the absence of microtubules is achieved through mechanical interactions (Wang et al., 2001) or via signaling pathways (Birukova et al., 2004; Chang et al., 2008; Kolodney and Elson, 1995; Verin et al., 2001).

Microtubules can signal to actomyosin through Rho family GTPases. RhoGTPases are key elements in the regulation of the actomyosin cytoskeleton in both cultured cells and during morphogenesis (Hall, 2005; Settleman, 2001). The Rho family members are well known to control cellular processes such as actin assembly, as well as the organization of myosin II-mediated contractility into lamellipodia and filopodia to guide cell migration and cell contractility. RhoGTPases can also regulate processes such as assembly of ECM (Dzamba et al., 2009) and the bulk elasticity of tissues through control of cortical actomyosin contractility and cell traction forces (Paszek et al., 2005). Thus, disrupting microtubules with drugs such as nocodazole may have inadvertently been testing not the role of microtubules but the role of RhoGTPases in development.

In this paper, we first investigate the contribution of microtubules to tissue stiffness and how microtubules indirectly repress tissue stiffening through the RhoGTPase guanine exchange factor GEF-H1 (Birkenfeld et al., 2008). We then use morpholino-based mRNA antisense to knock down the *Xenopus* homolog of GEF-H1, *Xlfc* (Kwan and Kirschner, 2005), revealing that microtubules have no direct role in maintaining bulk tissue stiffness but regulate actomyosin contractility indirectly. Large-scale defects in gastrulation generated by nocodazole can be partially but not completely rescued in morpholino-injected embryos, suggesting that nocodazole perturbs morphogenesis by two routes: the first by inhibiting RhoGEF-activity and the second through more conventional microtubule functions. This study identifies how cell-contraction phenomena typically studied in two-dimensions in cultured cells can manifest within functional three-dimensional tissues, i.e. embryos, as a macroscopic tissue stiffening.

MATERIALS AND METHODS

Embryos, explants, immunocytochemistry, and microscopy

Frog (*Xenopus laevis*) eggs were obtained through standard methods (Kay and Peng, 1991). Embryonic tissue explants for mechanical testing or high resolution imaging were microsurgically dissected after vitelline membranes were manually removed and embryos transferred to specially formulated culture media [Danilchik's For Amy or DFA (Sater et al., 1993)]. High-resolution images of GFP-tagged proteins in live tissues were collected using an $63\times/1.4N.A.$ oil immersion lens on an inverted compound microscope equipped with a confocal scanhead (SP5; Leica Microsystems, Bannockburn IL).

Capped mRNA was transcribed (Ampliscribe, Epicentre Biotech; Madison WI) from linearized expression plasmids. Approximately 0.5 to 1.0 ng of mRNA encoding a membrane-tagged GFP [mem-GFP (Wallingford et al., 2000)], an F-actin binding GFP [moe-GFP (Litman et al., 2000)] and microtubule-binding GFP [tau-GFP (Kwan and Kirschner, 2005)] were injected at the one-cell stage and fluorescently tagged proteins were expressed without effect on embryo development. Live embryonic tissues expressing fluorescent proteins were dissected from embryos between stages 10 and 10.5, and cultured on fibronectin-coated glass (20 $\mu\text{g}/\text{ml}$) in custom-made chambers designed for stable long-term confocal imaging.

Images of whole embryos and dorsal isolates were collected with a CCD-camera equipped stereomicroscope. Morphometric measurements were made using image analysis software (ImageJ v.1.38; Wayne Rasband,

National Institutes of Health). Statistical significance of treatments on morphometric measurements were determined using non-parametric Mann-Whitney *U*-tests for small sample sizes and Student's *t*-test for larger sample sizes (Sokal and Rohlf, 1994) using commercial statistical software (SPSS v. 15, Chicago, IL).

Measurement and analysis of mechanical properties

The nanoNewton force measurement device (nNFMD) is used to conduct uniaxial unconfined compressive stress-relaxation tests to measure the time-dependent viscoelastic properties of frog embryonic tissues (Davidson and Keller, 2007; Zhou et al., 2009). Briefly, the device measures the elastic modulus of regular blocks of dorsal axial tissues of uniform size, roughly 600 μm long and 400 μm wide. Tissues are positioned against a movable motor-controlled backstage and brought into contact with a force probe (Fig. 1C). To measure the residual tissue stiffness, tissues undergo 180-second stress-relaxation tests (Fig. 1D). A dorsal isolate is first compressed by 200 μm along its anterior-posterior axis and the resistive force of the tissue is collected by the force probe. After each test, the sample is immediately fixed in MEMFA (Sive et al., 2000) and the cross-sectional area is measured from the fixed explants using image analysis software (ImageJ v. 1.38). The strain experienced in each sample is calculated from its original and final lengths measured from a time-lapse sequence of the tissue recorded with a CCD camera-equipped stereomicroscope. The Young's elastic modulus 180 seconds after compression, $E(180)$, is calculated by:

$$E = \frac{\text{stress}}{\text{strain}} = \frac{\sigma}{s} = \frac{\left(\frac{F}{A}\right)}{\left(\frac{\Delta L}{L_0}\right)},$$

where E is the time dependent elastic modulus, F is the resistive force measured during the stress-relaxation test, A is the cross-sectional area, L_0 is the length of samples before compression and $\Delta L (=L_0 - L_{180})$ is the change of length before and after compression. Compressive forces are applied to the dorsal isolate along the anterior-posterior axis. Owing to the relative incompressibility of dense multicellular tissues, we expect compressive forces are converted to tensional forces along the mediolateral axis. Statistical significance of treatments on $E(180)$ for each clutch was carried out using the non-parametric Mann-Whitney *U*-test (Sokal and Rohlf, 1994) using commercial statistical software (SPSS v. 15). Statistical significance of treatments on $E(180)$ over a set of different clutches was carried out using one-way ANOVAs of log transformed data (Sokal and Rohlf, 1994). Log transformations were carried out to account for increased levels of variance as $E(180)$ increases. Throughout this paper we use the term 'stiffness' to mean the time-dependent elastic modulus reported at the end of a three-minute stress-relaxation test.

Manufacture of force-reporting gel substrates

In order to track the traction generated by mesodermal cells within marginal zone explants, we constructed soft fibronectin-conjugated polyacrylamide gel (FN-PAG) substrates embedded with fluorescent beads (Leach et al., 2007). Briefly, we first assembled a pre-mix with final concentration of 5% acrylamide, 0.05% bis-acrylamide, 0.1 $\mu\text{g}/\mu\text{l}$ bovine plasma fibronectin and dark red beads (43 nm diameter FluoSpheres; Invitrogen, Carlsbad CA) in phosphate-buffered saline (PBS). The ratio of acrylamide to bis-acrylamide was chosen to produce a gel of ~ 1000 Pa (Beningo and Wang, 2002) and confirmed by rheological tests (AR2000; TA Instruments, New Castle DE). The pre-mix solution was de-aerated under house vacuum for 20 minutes to remove oxygen from the solution. Then, N,N,N',N' -tetramethylethylenediamine (TEMED, Sigma-Aldrich), 0.01 $\mu\text{g}/\mu\text{l}$ acrylic acid *N*-hydroxysuccinimide (Sigma-Aldrich) and freshly made 0.4 $\mu\text{g}/\mu\text{l}$ ammonium persulfate (APS, Sigma-Aldrich) were added to make the pre-polymer mix. Pre-polymer (4 μl) was dispensed on clean cover slip and covered by a small 7×11 mm coverslip fragment. The thickness of gels cast in this geometry was measured by confocal microscopy in each experiment and averaged 59 μm , ranging from 35 to 88 μm . The FN-PAG polymerized in a humid nitrogen chamber for 30 minutes at room temperature. Following polymerization, the coverslip

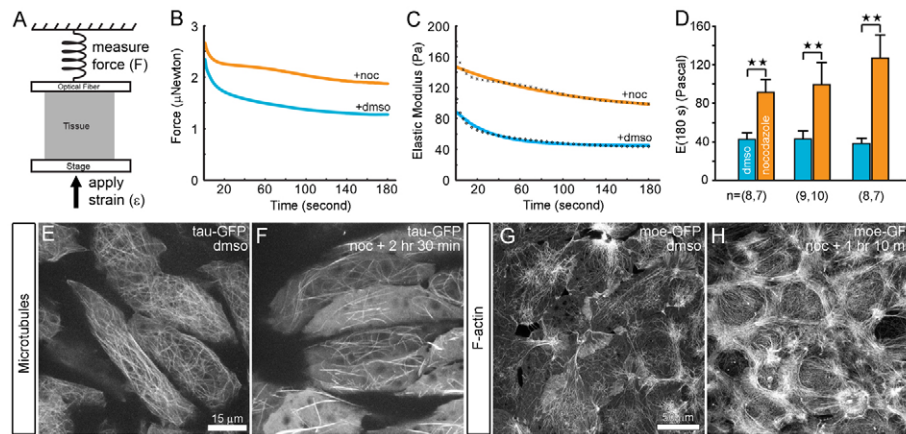


Fig. 1. Nocodazole stiffens embryonic tissues. (A) The elastic stiffness of early neural groove stage dorsal isolates (stage 16) are measured using a uniaxial unconfined compression test. (B) Representative plots of forces generated by two explants as they resist compression beginning at 0 seconds (blue line indicates explant incubated in DMSO; orange line indicates explant culture 40 minutes in 50 μ M nocodazole). (C) Representative time-dependent elastic modulus of the two explants are calculated from the forces measured in B, the initial strain imposed on each isolate, and the transverse cross-sectional area of each isolate. Broken lines indicate the viscoelastic standard linear solid model fitted to the time-dependent modulus. (D) Residual elastic or Young's modulus, $E(180)$, of 7 to 10 samples tested over three clutches or cohorts show nocodazole induces highly significant stiffening of dorsal isolates. We use the term 'stiffness' for convenience when referring to $E(180s)$. Double asterisks indicate highly significant differences ($P < 0.01$). (E) Tau-GFP expressed in mesodermal cells in marginal zone explants reports the presence of microtubules and (F) that nocodazole reduces the amount of microtubules. (G,H) Moe-GFP expressed in mesodermal cells in marginal zone explants reports (G) the presence of F-actin and (H) that nocodazole-treatment leads to increased amounts of F-actin over the same timescale.

fragment was carefully removed in 1/3×MBS solution and the FN-PAG washed in 1/3×MBS. The FN-PAG was used either immediately or stored for overnight in 1/3×MBS at 4°C.

Registration-based analysis of cell- and tissue-generated traction

In order to quantify relative amounts of traction produced by cells within mesodermal tissues, we adapted methods for culturing explants on force-reporting polyacrylamide gels (FN-PAG described above). Cell traction forces are often calculated from the displacements of individual beads bound within an ECM-conjugated polyacrylamide gel (Kandow et al., 2007); however, rather than track individual beads we used a method to track the displacement of parcels of gel using registration-based image analysis (Arganda-Carreras et al., 2006). Briefly, two-channel confocal time-lapse sequences were collected of cells within tissues expressing a membrane-targeted GFP cultured on a FN-PAG. Images of both GFP-labeled cells and dark-red fluorescing beads embedded within the gel were collected at the same plane-of-focus at the top-most surface of the FN-PAG. Preliminary tests revealed that individual beads or parcels of FN-PAG undergo periodic movements as cells appear to grab, move and then release the gel (data not shown). In order to determine the magnitude of traction forces exerted by cells within a tissue explant, we chose to measure gel displacements from the start of the time-lapse sequence rather than from a cell-free state of the gel (Beningo and Wang, 2002). Registration analysis calculates a displacement field needed to bring two images into alignment (Arganda-Carreras et al., 2006). The displacement field includes both x - and y -displacements for each pixel in the original image and the distribution of traction forces can be evaluated like any intensity-based image (Russ, 1999). We use the term 'traction map' to refer to an image representing the absolute displacement of gel substrate, without directional information, produced by cells.

RESULTS

As part of a continuing screen of candidate factors thought to modulate the stiffness of embryonic tissues, we tested the contribution of microtubules. As microtubules have long been implicated as key mechanical elements in cytoskeletal networks (Gardel et al., 2008) and key structural elements during morphogenesis (Burgess and Schroeder, 1979; Lane and Keller,

1997; Lee and Harland, 2007; Priess and Hirsh, 1986; Schoenwolf and Smith, 1990; Solnica-Krezel and Driever, 1994), we wanted to test the role of microtubules in establishing the mechanical properties of embryonic tissues.

Reducing microtubule density increases stiffness in frog embryonic tissues

We incubated dorsal isolates for 30-60 minutes in 50 μ M nocodazole, an inhibitor of microtubule polymerization (Keller et al., 1984; Lee and Harland, 2007; Tomasek and Hay, 1984), and used previously developed techniques to measure the time-varying elastic modulus of tissues microsurgically isolated from gastrulating frog embryos (Zhou et al., 2009). To measure these properties, we removed dorsal axial tissues from embryos that had successfully completed the first phase of gastrulation and were actively elongating (co-cultured whole embryos at stage 16). We subjected these explants to a uni-axial unconfined compression test along their anterior-posterior axis (Fig. 1A). Compressed explants resist with a force directed in the opposite direction that peaks within seconds and relaxes over 180 seconds (Fig. 1B). After 180 seconds, the dorsal explant is removed, fixed and bisected to measure its cross-sectional area. From the resistance force generated by the dorsal isolate and its cross-sectional area, we calculated an approximate time-varying elastic modulus, $E(t)$, for each explant (Fig. 1C). Tissue explants deform in response to applied forces in a manner consistent with viscoelastic materials (Findley et al., 1989) and soft biomaterials (Levental et al., 2007; Vincent, 1990; Wainwright et al., 1976). During compression the viscous response dissipates to reveal a long-term elastic response to compression. We compared this long-term elastic response (referred to here as 'stiffness') between sets of explants from the same mating to allow comparison of different treatments while minimizing the normal variation that occurs from clutch-to-clutch (von Dassow and Davidson, 2009; Zhou et al., 2009). Explants incubated for 30 to 60 minutes in 50 μ M nocodazole were

significantly stiffer, by two- to threefold, than explants incubated in DMSO carrier (Fig. 1D; 24 nocodazole-treated dorsal isolates and 24 DMSO-treated dorsal isolates from three clutches). Longer treatment or increased doses of nocodazole continued to increase the stiffness but to a diminishing degree (data not shown). To confirm that nocodazole reduced the density of microtubules, we visualized microtubules in living *Xenopus* explants using high resolution confocal time-lapse microscopy of explants expressing tau-GFP [Fig. 1E,F (Kwan and Kirschner, 2005)]. High doses of nocodazole did not completely eliminate microtubules but reduced their abundance, in agreement with previous studies (Kwan and Kirschner, 2005; Lane and Keller, 1997).

As previous studies found that tissue stiffness could be strongly influenced by actomyosin, we checked whether F-actin density was altered. To visualize live F-actin, we injected mRNA encoding moe-GFP into one-cell stage embryos, prepared tissue explants at gastrula stage and collected time-lapse sequences of cells within explants incubated with DMSO carrier or 50 μ M nocodazole (see Movies 1 and 2, respectively, in the supplementary material). Dense F-actin bundles assembled within 70 minutes of nocodazole treatment (Fig. 1G,H). We confirmed the live-cell imaging with fixed samples labeled with bodipy-FL phalloidin (data not shown). Previous efforts in our lab to directly enhance tissue stiffness by increasing F-actin polymerization or enhancing actomyosin contraction with compounds such as jasplakinolide and calyculin A, respectively, had failed, so we were surprised by the effects of nocodazole.

Tissue stiffening is due to RhoGEF activity

Increased levels of F-actin in fibroblasts incubated in nocodazole have been reported previously by Danowski (Danowski, 1989) and appear to be mediated by a microtubule-associated guanine exchange factor RhoGEF-H1 (Chang et al., 2008; Krendel et al., 2002). Xlfc, a *Xenopus laevis* homolog to RhoGEF-H1, has been previously cloned and implicated in gastrulation movements in *Xenopus* (Kwan and Kirschner, 2005) so we used antisense morpholinos to knock-down Xlfc (Xlfc-MO). Xlfc-MO reduced the effect of nocodazole on tissue stiffness when compared with control morpholino-injected explants treated with nocodazole (Fig. 2A). Xlfc-MO itself has no effect on tissue stiffness (see Fig. S1 in the supplementary material). The model for RhoGEF-H1 function proposed by Bokoch and co-workers (Birkenfeld et al., 2008; Chang et al., 2008) suggests that, when bound to microtubules, RhoGEF H1 is inactive; however, once released from microtubules, RhoGEF H1 activates RhoA (Chang et al., 2008). To test this model, we first confirmed that Xlfc-MO reduced the level of nocodazole-induced F-actin assembly in *Xenopus* explants (Fig. 2B,B',C,C'). We then confirmed that the stiffness inducing activity of nocodazole-released Xlfc could be recapitulated by the point-mutant Xlfc C55R, a constitutively active GEF (Kwan and Kirschner, 2005). Whole embryos expressing Xlfc C55R at high doses showed severe defects similar to those seen after overexpression of activated RhoGTPase (Tahinci and Symes, 2003) (data not shown). Reliable tissue explants could not be prepared from these embryos so we lowered the amount of Xlfc C55R mRNA injected to 175 pg per embryo, which allowed the majority of embryos to gastrulate successfully (Fig. 2D). Tissues isolated from these embryos showed significant stiffening: up to twofold greater than un-injected controls (Fig. 2E). Furthermore, like nocodazole-incubated tissues, stiffening was accompanied by sharp increases in F-actin in explants expressing moe-GFP (see Fig. S2 and Movie 3 in the supplementary material). Thus, the RhoGEF activity of Xlfc is both necessary and sufficient to induce stiffening and enrich F-actin in dorsal explants.

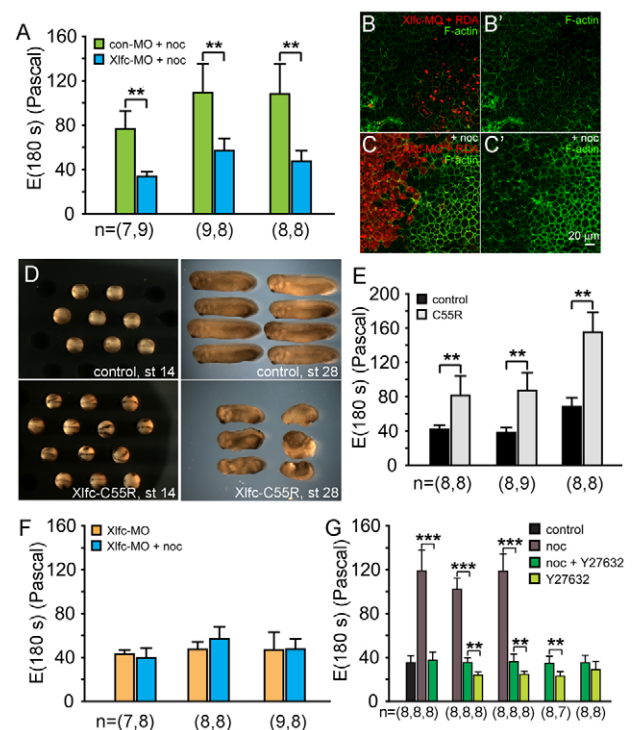


Fig. 2. Xlfc is both necessary and sufficient to stiffen dorsal isolates and induce F-actin assembly, and acts in part through Rho kinase. (A) Xlfc knock-down (Xlfc-MO) reduces nocodazole-induced stiffening of dorsal isolates. (B) Embryos with one blastomere injected at the four-cell stage with Xlfc-MO and rhodamine dextran amine (RDA) show no changes in endogenous F-actin levels. (B') F-actin levels alone in same field as in B. (C) Endogenous F-actin levels increase in the uninjected side once embryos are incubated with 50 μ M nocodazole. (B' and C' show levels of F-actin without RDA-labeled channels of B and C, respectively.) (D) Embryos expressing low quantities of the constitutively activated Xlfc point-mutant Xlfc-C55R close their blastopore but form dorsally shortened embryos. (E) Dorsal isolates from Xlfc-C55R-expressing embryos are twofold stiffer than controls. (F) Microtubules do not contribute to stiffness. Xlfc-MO injected embryos treated with and without nocodazole show that microtubules do not contribute directly to stiffness. (G) Nocodazole-induced stiffening is reduced by the Rho kinase inhibitor Y27632. Stiffness measurements of dorsal isolates incubated in DMSO carrier, 50 μ M nocodazole, and nocodazole and 40 μ M Y27632 show stiffness is restored to normal control levels after nocodazole and Y27632 are combined ($P < 0.01$; one clutch). Stiffness of isolates from three clutches show stiffness of nocodazole-treated tissues are significantly reduced after Y27632 treatment. Additional trials from four clutches treated with both 50 μ M nocodazole and 40 μ M Y27632 are also significantly stiffer than those treated with Y27632 alone. Comparisons of dorsal isolate stiffness within each clutch are tested for significance using the Mann-Whitney *U*-test and significance of stiffness measurements among multiple clutches were calculated using one-way ANOVA (** $P < 0.01$; *** $P < 0.005$).

Microtubules do not contribute to tissue stiffness

To test whether Xlfc-induced contractility could be obscuring a genuine contribution of microtubules to tissue stiffness, we tested the role of microtubules in dorsal isolates prepared from embryos where Xlfc synthesis had been knocked down. As previously reported, Xlfc-MO knock down has little effect on early *Xenopus*

morphogenesis (Kwan and Kirschner, 2005). We found Xlfc-MO injected explants showed no change in stiffness once microtubules were depolymerized (Fig. 2F).

We next wanted to test whether increased levels of microtubules could alter tissue stiffness. To increase microtubule density within dorsal isolates, we used taxol: a drug that stabilizes microtubules (Schiff et al., 1979) and can increase the stiffness of individual microtubules (Gittes et al., 1993). Short-term treatment of marginal zone explants expressing tau-GFP resulted in modest increases in microtubule density without altering the overall distribution of microtubules observed in DMSO-control treated explants (see Fig. S3A in the supplementary material). Dorsal isolates incubated 60 to 90 minutes in 23 μ M taxol showed no significant differences in stiffness from control isolates cultured in DMSO (see Fig. S3 in the supplementary material). Long-term incubation in taxol produces large aster-like microtubule structures (see Fig. S3C in the supplementary material) that have been described previously (Lee and Harland, 2007). Together, our findings indicate that microtubules do not contribute to the stiffness of *Xenopus* embryonic dorsal tissues.

RhoGEF-mediated stiffening acts through myosin II

RhoGEF activated RhoGTPase could influence tissue stiffness by altering F-actin polymerization (Watanabe et al., 1999), by enhancing the bundling of filaments (Machesky and Hall, 1997), or by enhancing myosin II contractility (Somlyo and Somlyo, 2000). As our previous work found that we could reduce tissue stiffness with a drug that acutely inhibited Rho kinase to reduce myosin II activity, we used same drug, Y27632, to see whether nocodazole-induced tissue stiffening was due to actomyosin contractility. Incubation of dorsal isolates for 60 minutes in 50 μ M nocodazole and 40 μ M Y-27632 reduced the stiffness of nocodazole-treated tissues to control levels (one clutch, Fig. 2G) and addition of Y27632 consistently reduced stiffness of nocodazole treated isolates ($P=0.001$, three clutches; Fig. 2G). We also found a consistent and significant increase in stiffness in explants incubated in nocodazole and Y27632 compared with those incubated in only Y27632 ($P=0.004$, four clutches; Fig. 2G). To test the effectiveness of Y27632 in reducing myosin II function, we carried out immunofluorescence staining of dorsal isolates with an antibody recognizing phospho-myosin regulatory light chain (pMLC). We found high levels of pMLC in prospective somite and notochord, and low levels within the endoderm (see Fig. S4A,E in the supplementary material). As expected, Y27632 significantly reduced levels of phospho-MLC in the prospective somitic mesoderm (see Fig. S4B,F in the supplementary material). Surprisingly, parallel studies using 100 μ M blebbistatin, an inhibitor of myosin heavy chain (Straight et al., 2003), had no effect on tissue stiffness (data not shown; 18 control versus 16 treated from two clutches). The reason for differences between the effects of Y27632 and blebbistatin are not entirely clear but blebbistatin can break down rapidly in light (Sakamoto et al., 2005). Taken together, these results suggest myosin II is a major effector in tissue stiffening.

These results support a role for myosin contractility but do not rule out a role for increased levels of F-actin within the cortex of nocodazole-treated mesoderm cells. As RhoGTPases can alter levels of F-actin (Ridley, 2006), we tested the effectiveness of 0.6 μ M Latrunculin B (LatB) in reducing the effect of nocodazole. As in previous work (Zhou et al., 2009), we found 0.6 μ M LatB could reduce stiffness of nocodazole-treated isolates by 35% (nocodazole,

118 \pm 19 Pa, $n=8$; nocodazole with LatB, 42 \pm 23 Pa, $n=7$). Furthermore, consistent with our initial findings, nocodazole can still increase stiffness of LatB-incubated isolates by 2.5-fold (LatB, 31 \pm 8 Pa, $n=8$; LatB and nocodazole, 77 \pm 28 Pa, $n=7$). These analyses cannot rule out a contribution of actin bundling or additional F-actin polymerization in nocodazole-induced tissue stiffening; however, the principle effects of nocodazole on tissue stiffness can be blocked at the level of myosin II activity.

MT depolymerization activates cell contraction to stiffen the tissue

Danowski (Danowski, 1989) observed single fibroblasts became much more contractile after treatment with nocodazole and we wondered whether nocodazole-treated *Xenopus* cells within tissues behaved similarly. The early experiments carried out by Harris and colleagues qualitatively assessed cell-generated traction forces by observing wrinkling of thin silicone sheets with adherent cells (Harris et al., 1980). In order to determine whether *Xenopus* cells incubated in nocodazole exhibited similar increased forces of contractility, we turned to culturing tissue explants on force reporting polyacrylamide gels. Such gels and other mechanically deformable substrates have been used primarily to observe traction forces of individual cells (Beningo et al., 2002) and to control substrate stiffness for investigations of the role of the physical micro-environment on cell behavior (Solon et al., 2007) or differentiation (Engler et al., 2006). Such force-reporting gels have been used to study traction forces in multicellular tissues formed by migrating *Dictyostelium* slugs (Barentin et al., 2006; Rieu et al., 2005) and beneath static (Li et al., 2009) and migrating sheets of cultured cells (Treat et al., 2009). Stiffer substrates, such as polydimethylsiloxane, have been used to measure traction forces required for the assembly of fibronectin fibrils beneath *Xenopus* animal cap cells (Dzamba et al., 2009). We would prefer to investigate cell traction on gels that were as stiff as tissues found in the embryo at these stages; however, we were unable to consistently synthesize polyacrylamide gels in the range of 10 to 100 Pa. Instead, we chose to investigate traction on stiffer substrates so we cast 0.05% bis-acrylamide/polyacrylamide gels together with fibronectin to provide a flexible adhesive substrate. This mixture consistently produces gels with elastic modulus of \sim 1000 Pa (Kandow et al., 2007). Small fluorescent beads were copolymerized with the gel to allow detection of small deformations within the gel. Marginal zone explants harvested from early gastrula stage embryos expressing a mem-GFP were cultured on the gel (Fig. 3A) for 1 hour before either DMSO or 50 μ M nocodazole was added to the media. Cell behaviors and bead movements were tracked using confocal time-lapse microscopy (Fig. 3B). One hour later, mem-GFP (Fig. 3C) and red-fluorescent microsphere beads (Fig. 3D) at the surface of the gel (Fig. 3D) were followed in single confocal sections collected at 60-second intervals (cell and bead movements after treatment in DMSO and nocodazole can be seen in Movies 4 and 5, respectively, in the supplementary material).

Resolving traction under *Xenopus* explants undergoing morphogenesis required development of a novel approach. Conventional approaches to measuring traction forces generated by cultured cells or small numbers of *Xenopus* embryonic cells involve identification and tracking of individual beads and the removal of the cell or tissue at the conclusion of the experiment to obtain bead positions for the 'zero-force' state (Beningo et al., 2002; Dzamba et al., 2009; Treat et al., 2009). Comparing 'zero-force' bead positions with the positions of beads under live explants is made very difficult

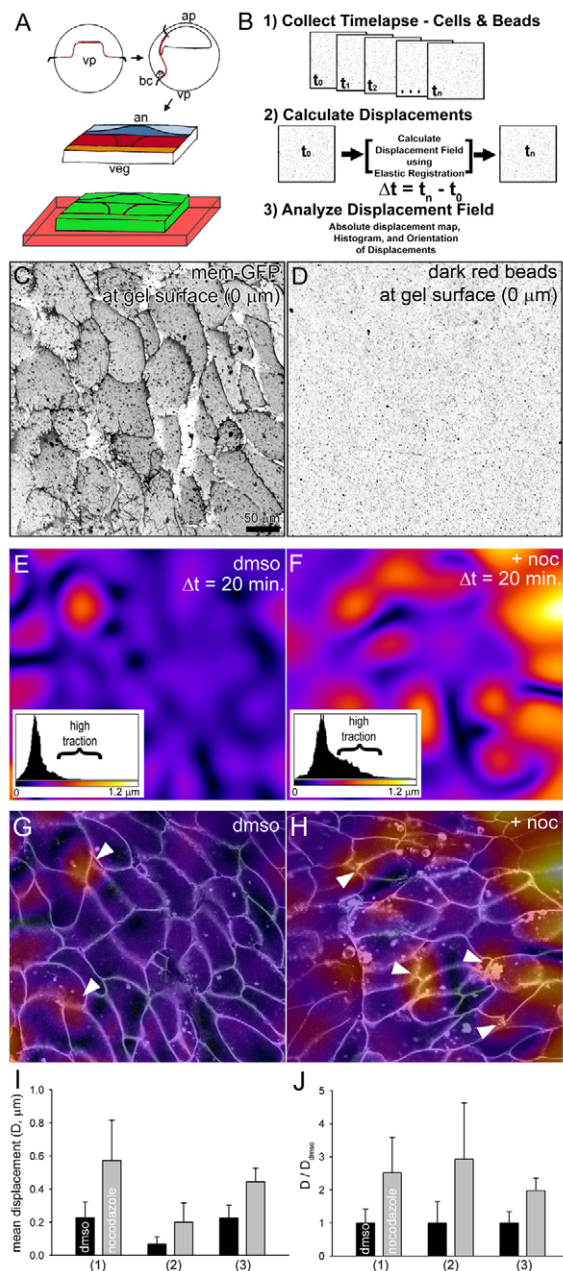


Fig. 3. Traction maps reveals nocodazole increases physical contractility of tissue. (A) Assembly of marginal zone explants on displacement-reporting polyacrylamide gels. (B) Traction maps are calculated from confocal time-lapse sequences of gel, cell and tissue movements. (C) Confocal section of mesodermal cells expressing a mem-GFP cultured on fibronectin-conjugated polyacrylamide gel. (D) Confocal section collected at the same level shows the position of dark-red fluorescent microspheres beads on the surface of the gel. (E) Traction map shows the magnitude of bead displacements beneath mesodermal cells within an intact marginal zone explant incubated in DMSO. The inset histogram shows the frequency of bead displacements and the scale of displacements. Most displacements are limited to less than 0.3 μm within the color range of purple to blue; regions of high traction above 0.3 μm are within the color ranges of red to yellow. (F) Traction map of mesodermal cells in explants incubated in 50 μM nocodazole show large displacements spread over larger areas. The histogram shows a large increase in regions of high traction. (G,H) Combined displacement maps shown in E and F, respectively, with overlying cells outlines collected from a confocal section 5 μm deeper into the cells. High regions of traction in both DMSO and after incubation in nocodazole appear to colocalize with cell-cell junctions at the mediolateral ends of cells (arrowheads). (I) Mean displacements calculated from the full field of view collected from three explants from three clutches show significant and large increases in traction after explants are incubated in nocodazole. Variances from clutch to clutch may reflect slight changes in substrate preparation or clutch-to-clutch differences in cell-generated traction. (J) Mean displacements normalized for each clutch show nocodazole consistently increases traction in all cases.

owing to morphogenetic movements within cultured *Xenopus* explants. Coordinated cell movements in *Xenopus* explants can take several hours to become reliable after tissues are microsurgically removed. During that time, tissue movements begin to reshape the explant (Davidson et al., 2004) and generate both microscopic forces under cells and macroscopic forces both in the plane and out of the plane of the explant (J.Z. and L.A.D., unpublished). Removing *Xenopus* tissues not only releases cells from the substrate but also releases the macroscopic forces throughout the explant. Thus, to measure traction forces, we turned to developing a method that would allow us to identify temporal changes in traction.

Temporal changes in traction are more relevant to the dynamic micro-environment of intercalating mesodermal cells. *Xenopus* embryonic cells move and extend protrusions in a punctuated manner. Preliminary analyses of beads showed that they too undergo punctuated cycles of movement interspersed with

quiescent periods. To analyze temporal changes in traction over an entire field of cells, we developed a quantitative method based on image registration (Arganda-Carreras et al., 2006) for measuring the absolute displacements of the gel. This method allows visualization of displacements to be combined with confocal sections collected from explants expressing mem-GFP. To validate this method, we assessed the algorithm used to measure traction under nocodazole-treated explants (Fig. 3, see Fig. S5A,B in the supplementary material) in null-force conditions (see Fig. S5C in the supplementary material), with two random bead images (see Fig. S5D in the supplementary material), and after point forces have been applied to the surface of a gel by a mechanical probe (see Fig. S5E,F in the supplementary material). Thus, the image registration method allows us to compare temporal patterns of traction generated within an entire field of cells.

Traction generated by a field of mediolaterally intercalating mesodermal cells in marginal zone explants was quantified using the image registration method. Image registration produces a pixel-by-pixel map of cell tractions based on the direction and magnitude of movements in the gel substrate beneath multicellular tissues. From this map, we can visualize the degree of substrate movement beneath intercalating cells and using histograms we can quantify areas of high contraction. DMSO-treated control explants containing elongating mesodermal cells generated heterogeneous patterns of traction over 20 minutes (Fig. 3E). However, identically staged elongating mesoderm cells in nocodazole-treated explants generated greater traction over a much larger area (Fig. 3F). To quantify the changes in high-traction areas, we compared histograms of traction maps from DMSO controls with their matching nocodazole-treated traction maps. Traction maps from control explants show 10% of the map exhibits displacements

greater than $0.34 \mu\text{m}$. By contrast, after incubating with nocodazole more than 67% of the traction map shows traction greater than $0.34 \mu\text{m}$ displacement. Thus, nocodazole causes high traction areas to increase from 10% to 67% (i.e. a 6.7-fold increase). Similar analysis reveals areas covered by the highest levels of traction expand to 53% (set 2) and 77% (set 3) of the total area under the explants. Thus, the areas with the highest tractions, covering 10% of the area in control explants, expanded in area 6.7-, 5.3- and 7.7-fold after nocodazole treatment. Traction maps combined with confocal images of cell shape reveal that traction-mediated bead displacement is highest at sites of cell-cell junctions localized at the mediolateral ends of intercalating cells (arrowheads; Fig. 3G,H). Analysis of mesodermal cells in explants from three different clutches of embryos reveals some differences in base levels of traction (Fig. 3I) but all cases show that nocodazole induces substantially higher mean traction than control explants (Fig. 3J). Thus, nocodazole treatment activates Xlfc RhoGEF, increases cell traction or contractility and stiffens dorsal tissues.

Mechanical rescue: developmental defects caused by nocodazole treatment can be reduced by Xlfc knock down

The microtubule cytoskeleton plays diverse roles from involvement in mitosis and directed vesicular transport to involvement in cell mechanics during epithelial morphogenesis. Among their mechanical roles, microtubules have been suggested to operate like compressive struts (Wang et al., 2001) that elongate cells or to provide mechanical support for columnar or bottle-shaped cells (Lee and Harland, 2007). Many of these hypotheses have been based on observations of embryos after colchicine- or nocodazole-induced disruption of microtubules (e.g. Burnside, 1975). From our findings, we wondered whether these defects might instead be due to the defects in other functions of microtubules rather than due to the RhoGEF Xlfc-mediated activation of myosin II contractility (Fig. 4A).

To test the role of microtubules and separate their function from the role of myosin II contractility we attempted to ‘mechanically-rescue’ nocodazole-induced or RhoGEF-induced contractility during blastopore closure. We chose blastopore closure as it is the first large-scale movement of morphogenesis that can be perturbed by nocodazole (Lane and Keller, 1997; Lee and Harland, 2007) and is similarly perturbed by expression of the constitutively activated RhoGEF Xlfc-C55R (Fig. 4B). Treatment of early gastrula stage (stage 10 1/4 to 10 1/2) embryos with more than $50 \mu\text{M}$ nocodazole slows or blocks blastopore closure as previously reported (Kwan and Kirschner, 2005; Lane and Keller, 1997). As earlier studies from our lab found that the Rho Kinase inhibitor Y27632 could reliably reduce tissue stiffness by 50% without altering the overall progress of gastrulation [a 50% reduction of stiffness appears to be within the range of variability allowing successful gastrulation in *Xenopus* embryos (von Dassow and Davidson, 2009)], we wondered whether the contrary effects of nocodazole and Y27632 could rescue the process of blastopore closure. To test this, we cultured batches of 25 to 30 early gastrula stage embryos in $30 \mu\text{M}$ nocodazole combined with increasing concentrations of 10, 40 and $100 \mu\text{M}$ Y27632. Control embryos were cultured with DMSO carrier alone, $30 \mu\text{M}$ nocodazole alone and $100 \mu\text{M}$ Y27632 alone. Nocodazole treatment at this stage severely blocks blastopore closure. We found that Y27632 could not rescue the effects of nocodazole (data not shown). To further distinguish the role of microtubules, we investigated blastopore closure in embryos with reduced levels of Xlfc incubated in nocodazole (Fig. 4A-C). In this case, embryos injected with Xlfc-MO and cultured in $30 \mu\text{M}$

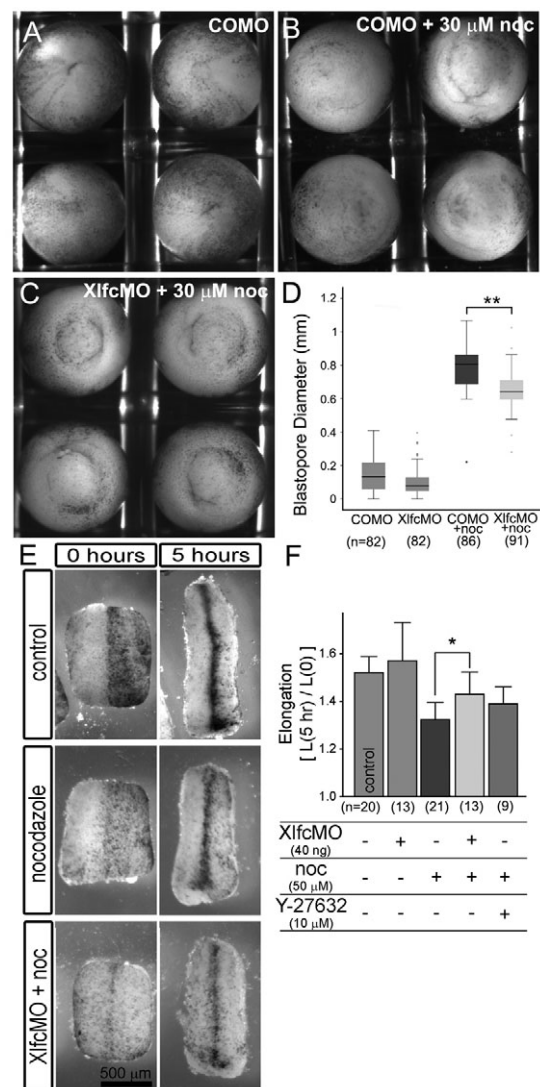


Fig. 4. Mechanical rescue of developmental defects. (A-D) Xlfc-MO produces a small but significant rescue of blastopore closure defects induced by nocodazole. (E,F) Xlfc-MO produces a moderate rescue of dorsal isolate elongation rates. (A) Embryos injected with control morpholinos close their blastopore. (B) Control morpholino-injected embryos cultured from stage 10.25 onwards in $30 \mu\text{M}$ nocodazole do not close their blastopore. (C) Embryos injected with Xlfc MO show some improvements in closing their blastopore. (D) Measurements of the diameter of the open-blastopore at stage 12.75 (just prior to closure in control embryos) show Xlfc MO provides a small but highly significant rescue of the nocodazole-induced open blastopore defect. (E) Dorsal isolates cultured from stage 13 onwards extend by nearly 50%. Incubation in $50 \mu\text{M}$ nocodazole reduces the degree of elongation, but prior injection with Xlfc MO can ameliorate that reduction. (F) Quantitative measurements of explants from three different clutches show that prior injection with XlfcMO can partly rescue the nocodazole-induced effects. By contrast, low doses of Y27632 do not provide significant rescue.

nocodazole showed small but significant improvement in the degree of blastopore closure over control MO-injected embryos cultured in nocodazole ($P < 0.01$; Student's *t*-test; Fig. 4D). However, blastopore closure was still significantly perturbed compared with control embryos.

As Xlfc knock down and incubation with Y27632 had been reported to rescue early stage elongation of Keller sandwich explants (Kwan and Kirschner, 2005), we investigated whether late stage elongation of dorsal isolates could also be rescued by these treatment. We found that 50 μ M nocodazole significantly slowed dorsal isolate elongation by 38% (Fig. 4E). Knocking down Xlfc reduced the effect of nocodazole but did not restore the full elongation rate. In contrast to the reported rescue of nocodazole-treated sandwich explants using Y27632, we found a slight but not statistically significant improvement in elongation after incubating dorsal isolates in 50 μ M nocodazole and 10 μ M Y27632 (Fig. 4F). In summary, effects of nocodazole on tissue stiffness can be rescued by inhibiting myosin II activity with a Rho Kinase inhibitor or knocking-down Xlfc synthesis with anti-Xlfc morpholinos. By contrast, the gross morphogenetic defects induced by nocodazole are only moderately rescued by knocking down Xlfc or by inhibiting myosin contractility.

DISCUSSION

We found that microtubule depolymerization increases dorsal tissue stiffness in *Xenopus* via a RhoGTPase-mediated activation of actomyosin contractility. Nocodazole effects on mechanical properties are due primarily to the activation of cell contractility by RhoGEF-H1 and are blocked by morpholinos that knock down synthesis of the *Xenopus* homolog Xlfc. Our results extend earlier observations that microtubules repress single cultured cell contractility and that cell contractility can regulate embryonic tissue stiffness. These same reagents have been previously used to investigate the role of Xlfc and nocodazole in controlling polarized cell behaviors during convergent extension (Kwan and Kirschner, 2005) and we have shown that they also alter the mechanical microenvironment and globally increase levels of cell contractility. In light of our findings, we suggest a re-evaluation of the role of microtubules in regulating both cell behaviors and the mechanics of morphogenetic movements because of the prevalent use of microtubule depolymerizing drugs such as nocodazole.

Connecting cellular force production, adhesion, traction, stiffness and morphogenesis

Few studies have used traction-reporting gels to study the roles of cell contraction and adhesion within multicellular tissues (Li et al., 2009; Trepap et al., 2009). In theory, increased levels of traction observed after nocodazole treatment could reflect contribution from both cell contraction (i.e. internal force generation) and adhesion to gel-bound fibronectin. For example, increased tractions could be achieved by increasing the number of focal adhesions or the force produced at each adhesion or some combination of the two. Our current studies with traction-reporting gels do not distinguish between these mechanisms; however, in combination with other findings reported here, we strongly suspect nocodazole increases the contribution of cell contraction. To resolve the relative contribution of cell adhesion to cell traction, future studies will be needed to identify discrete sites of cell adhesion, the direction and magnitude of force generation at these sites, and how efficiently cells within a tissue transmit intracellular forces to extracellular matrix or gel substrates.

Why should contraction stiffen tissues? The macroscopic changes in stiffness reflect underlying changes in actomyosin dynamics. These observations suggest that pathways regulating cell-contraction or force-generating programs could alter the macroscopic biomechanical properties of tissues and in turn direct subsequent cell behaviors because of altered micro-environments.

As a first approximation, it can be useful to think of a cell or tissue as an actin gel. The mechanics of reconstituted actin gels depend crucially on three factors: the concentration of actin, the number of cross-linkers between actin filaments and the activity of myosin cross-linkers (Gardel et al., 2006; Koenderink et al., 2009). Thus, the more contractile the embedded myosin motors the stiffer the gel becomes. Thus, there is no single linear pathway that controls physical mechanics; instead, mechanical properties are derived from diverse cellular processes ranging from cell adhesion to the physical properties of the cytoskeleton.

Molecular contribution of the cytoskeleton to embryonic tissue stiffness

In a previous study, we characterized stiffness changes in the embryo that accompany stage and identity of differentiating germ-layers, ruled out a contribution of fibrillar fibronectin ECM, and implicated actomyosin in regulating stiffness in early neural plate stage embryos (Zhou et al., 2009). Many of our treatments, such as disrupting actin polymerization or inhibiting myosin II contractility, reduced stiffness by 50%. However, factors that have been reported to stabilize F-actin or enhance myosin II contractility did not increase the stiffness of embryonic tissues. It was surprising that severe disruptions of actomyosin resulted in relatively minor changes in tissue stiffness. Other elements of the cytoskeleton [such as intermediate filaments (Sivaramakrishnan et al., 2008)], factors that modify the cytoskeleton [such as actin crosslinking proteins (Esue et al., 2009)] and cell-cell adhesions that modulate cytoskeletal assembly (Nandadasa et al., 2009; Tao et al., 2007) are likely contributors to the eightfold changes in stiffness from stage-to-stage or the 10-fold changes from tissue-to-tissue. Future studies on the mechanical contribution of these processes will require more specific tools to perturb their function and characterize the consequences in the full context of the cytoskeleton and cellular architecture.

Considerable attention has been focused on the regulation of the cytoskeleton and cell motility through Rho family GTPases; however, this study demonstrates these same bi-molecular switches are also likely to regulate tissue stiffness. Thus, Rho family and perhaps other Ras family GTPases and diverse regulatory factors [such as Xlfc, other GEFs, GTPase activating proteins (GAPs) and guanosine nucleotide dissociation inhibitors (GDIs)] could play major roles in controlling and modulating both cellular and tissue-scale mechanics within developing embryos and organs. As Xlfc-MO has no effect on tissue stiffness and does not perturb *Xenopus* development, it is unlikely that Xlfc regulates the stiffness changes observed in the *Xenopus* embryo (Zhou et al., 2009). RhoGEF H1/Lfc is involved in regulating cell contractility during mitosis (Bakal et al., 2005), spine formation during dendrite formation (Ryan et al., 2005) and is a gene target of TGF β signaling (Tsapara et al., 2010). Much work remains to identify these roles, whether they require reduced microtubule mass or other triggering mechanisms, using both in vitro and in vivo systems.

Re-evaluation of the role of microtubules in morphogenesis

We suggest a re-evaluation of the role of microtubules during morphogenesis because of the prevalent use of nocodazole in many studies. In vertebrates, nocodazole disrupts blastopore closure in frog (Lane and Keller, 1997; Lee and Harland, 2007), epiboly in zebrafish (Solnica-Krezel and Driever, 1994) and the epithelial-to-mesenchymal transition in chick gastrulation (Nakaya et al., 2008). Furthermore, nocodazole universally disrupts neurulation (Brun and Garson, 1983; Karfunkel, 1971; Karfunkel, 1972; Smedley and

Stannisstreet, 1986) and has been shown to disrupt events driven by epithelial folding such as formation of the lens in chick (Zwaan and Hendrix, 1973). We suspect the disruption of several of these morphogenetic movements may be due to elevated levels of actomyosin contraction or global stiffening of embryonic tissues. High levels of contractility may alter cell shapes, causing cells to shorten and round. Altered levels of cell surface contractility may also alter the capacity of cells to rearrange themselves (Krieg et al., 2008; Puech et al., 2005) or their ability to maintain tissue polarity (Ninomiya and Winklbauer, 2008). Global stiffening may result in tissues 'locking-up' or becoming too stiff for normal levels of force generation to bend or fold tissues. It is clear that the roles of microtubules are diverse in cells and during development, but future efforts will need a broader focus on the integrative mechanics and the contribution of different molecular, cellular and tissue-scale structures to the movements of morphogenesis.

Acknowledgements

We would like to thank members of the Davidson lab for providing critical comments on this paper. We especially thank Dr Michelangelo von Dassow for advice on statistical analysis, polyacrylamide gel preparation and lively discussions on robustness. We also thank Dr Kristen Kwan for comments on the manuscript; both Dr Kwan and Dr Marc Kirschner for Xlfc reagents and the tau-GFP plasmid; and Dr John Wallingford for providing us with the moe-GFP plasmid. This study was supported by grants from the National Institutes of Health (HD044750), the National Science Foundation (IOS-0845775) and an American Heart Association Beginning Grant-in-Aid to L.A.D. Deposited in PMC for release after 12 months.

Competing interests statement

The authors declare no competing financial interests.

Supplementary material

Supplementary material for this article is available at <http://dev.biologists.org/lookup/suppl/doi:10.1242/dev.045997/-/DC1>

References

- Arganda-Carreras, I., Sorzano, C. O. S., Marabini, R., Carazo, J. M., de Solorzano, C. O. and Kybic, J. (2006). Consistent and elastic registration of histological sections using vector-spline regularization. *CVAMIA: Computer Vision Approaches to Medical Image Analysis* **4241**, 85-95.
- Bakal, C. J., Finan, D., LaRose, J., Wells, C. D., Gish, G., Kulkarni, S., DeSepulveda, P., Wilde, A. and Rottapel, R. (2005). The Rho GTP exchange factor Lfc promotes spindle assembly in early mitosis. *Proc. Natl. Acad. Sci. USA* **102**, 9529-9534.
- Barentin, C., Sawada, Y. and Rieu, J. P. (2006). An iterative method to calculate forces exerted by single cells and multicellular assemblies from the detection of deformations of flexible substrates. *Eur. Biophys. J.* **35**, 328-339.
- Beningo, K. A. and Wang, Y. L. (2002). Flexible substrata for the detection of cellular traction forces. *Trends Cell. Biol.* **12**, 79-84.
- Beningo, K. A., Lo, C. M. and Wang, Y. L. (2002). Flexible polyacrylamide substrata for the analysis of mechanical interactions at cell-substratum adhesions. *Methods Cell Biol.* **69**, 325-339.
- Birkenfeld, J., Nalbant, P., Yoon, S. H. and Bokoch, G. M. (2008). Cellular functions of GEF-H1, a microtubule-regulated Rho-GEF: is altered GEF-H1 activity a crucial determinant of disease pathogenesis? *Trends Cell. Biol.* **18**, 210-219.
- Birukova, A. A., Smurova, K., Birukov, K. G., Usatyuk, P., Liu, F., Kaibuchi, K., Ricks-Cord, A., Natarajan, V., Alieva, I., Garcia, J. G. et al. (2004). Microtubule disassembly induces cytoskeletal remodeling and lung vascular barrier dysfunction: role of Rho-dependent mechanisms. *J. Cell Physiol.* **201**, 55-70.
- Brun, R. B. and Garson, J. A. (1983). Neurulation in the Mexican salamander (*Ambystoma mexicanum*): a drug study and cell shape analysis of the epidermis and the neural plate. *J. Embryol. Exp. Morphol.* **74**, 275-295.
- Burgess, D. R. and Schroeder, T. E. (1979). The cytoskeleton and cytomusculature in embryogenesis-an overview. *Methods Achiev. Exp. Pathol.* **8**, 171-189.
- Burnside, B. (1975). The form and arrangement of microtubules: an historical, primarily morphological, review. *Ann. NY Acad. Sci.* **253**, 14-26.
- Chan, C. E. and Odde, D. J. (2008). Traction dynamics of filopodia on compliant substrates. *Science* **322**, 1687-1691.
- Chang, Y. C., Nalbant, P., Birkenfeld, J., Chang, Z. F. and Bokoch, G. M. (2008). GEF-H1 couples nocodazole-induced microtubule disassembly to cell contractility via RhoA. *Mol. Biol. Cell* **19**, 2147-2153.
- Cojoc, D., Difato, F., Ferrari, E., Shahapure, R. B., Laishram, J., Righi, M., Di Fabrizio, E. M. and Torre, V. (2007). Properties of the force exerted by filopodia and lamellipodia and the involvement of cytoskeletal components. *PLoS ONE* **2**, e1072.
- Collinsworth, A. M., Zhang, S., Kraus, W. E. and Truskey, G. A. (2002). Apparent elastic modulus and hysteresis of skeletal muscle cells throughout differentiation. *Am J. Physiol. Cell Physiol.* **283**, C1219-C1227.
- Danowski, B. A. (1989). Fibroblast contractility and actin organization are stimulated by microtubule inhibitors. *J. Cell Sci.* **93**, 255-266.
- Davidson, L. and Keller, R. (2007). Measuring mechanical properties of embryos and embryonic tissues. *Methods Cell Biol.* **83**, 425-439.
- Davidson, L. A., Keller, R. and DeSimone, D. (2004). Patterning and tissue movements in a novel explant preparation of the marginal zone of *Xenopus laevis*. *Gene Expr. Patterns* **4**, 457-466.
- Davidson, L. A., Von Dassow, M. and Zhou, J. (2009). Multi-scale mechanics from molecules to morphogenesis. *Int. J. Biochem. Cell Biol.*
- Dennerli, T. J., Joshi, H. C., Steel, V. L., Buxbaum, R. E. and Heidemann, S. R. (1988). Tension and compression in the cytoskeleton of PC-12 neurites. II: Quantitative measurements. *J. Cell Biol.* **107**, 665-674.
- Dzamba, B. J., Jakab, K. R., Marsden, M., Schwartz, M. A. and DeSimone, D. W. (2009). Cadherin adhesion, tissue tension, and noncanonical Wnt signaling regulate fibronectin matrix organization. *Dev. Cell* **16**, 421-432.
- Engler, A. J., Sen, S., Sweeney, H. L. and Discher, D. E. (2006). Matrix elasticity directs stem cell lineage specification. *Cell* **126**, 677-689.
- Esue, O., Tseng, Y. and Wirtz, D. (2009). Alpha-actinin and filamin cooperatively enhance the stiffness of actin filament networks. *PLoS ONE* **4**, e4411.
- Findley, W. N., Lai, J. S. and Onaran, K. (1989). Creep and relaxation of nonlinear viscoelastic materials. New York: Dover Publications, Inc.
- Gardel, M. L., Nakamura, F., Hartwig, J. H., Crocker, J. C., Stossel, T. P. and Weitz, D. A. (2006). Prestressed F-actin networks cross-linked by hinged filamins replicate mechanical properties of cells. *Proc. Natl. Acad. Sci. USA* **103**, 1762-1767.
- Gardel, M. L., Kasza, K. E., Brangwynne, C. P., Liu, J. and Weitz, D. A. (2008). Chapter 19, Mechanical response of cytoskeletal networks. *Methods Cell Biol.* **89**, 487-519.
- Gittes, F., Mickey, B., Nettleton, J. and Howard, J. (1993). Flexural rigidity of microtubules and actin filaments measured from thermal fluctuations in shape. *J. Cell Biol.* **120**, 923-934.
- Hall, A. (2005). Rho GTPases and the control of cell behaviour. *Biochem. Soc. Trans.* **33**, 891-895.
- Harris, A. K., Wild, P. and Stopak, D. (1980). Silicone rubber substrata: a new wrinkle in the study of cell locomotion. *Science* **208**, 177-179.
- Janmey, P. A. (1991). Mechanical properties of cytoskeletal polymers. *Curr. Opin. Cell Biol.* **3**, 4-11.
- Janmey, P. A., Euteneuer, U., Traub, P. and Schliwa, M. (1991). Viscoelastic properties of vimentin compared with other filamentous biopolymer networks. *J. Cell Biol.* **113**, 155-160.
- Kandow, C. E., Georges, P. C., Janmey, P. A. and Beningo, K. A. (2007). Polyacrylamide hydrogels for cell mechanics: steps toward optimization and alternative uses. *Methods Cell Biol.* **83**, 29-46.
- Karfunke, P. (1971). The role of microtubules and microfilaments in neurulation in *Xenopus*. *Dev. Biol.* **25**, 30-56.
- Karfunke, P. (1972). The activity of microtubules and microfilaments in neurulation in the chick. *J. Exp. Zool.* **181**, 289-301.
- Kay, B. K. and Peng, H. B. (1991). *Xenopus laevis: Practical Uses in Cell and Molecular Biology*. New York: Academic Press.
- Keller, H. U., Naef, A. and Zimmermann, A. (1984). Effects of colchicine, vinblastine and nocodazole on polarity, motility, chemotaxis and cAMP levels of human polymorphonuclear leukocytes. *Exp. Cell Res.* **153**, 173-185.
- Koenderink, G. H., Dogic, Z., Nakamura, F., Bendix, P. M., MacKintosh, F. C., Hartwig, J. H., Stossel, T. P. and Weitz, D. A. (2009). An active biopolymer network controlled by molecular motors. *Proc. Natl. Acad. Sci. USA* **106**, 15192-15197.
- Kolodney, M. S. and Elson, E. L. (1995). Contraction due to microtubule disruption is associated with increased phosphorylation of myosin regulatory light chain. *Proc. Natl. Acad. Sci. USA* **92**, 10252-10256.
- Krendel, M., Zenke, F. T. and Bokoch, G. M. (2002). Nucleotide exchange factor GEF-H1 mediates cross-talk between microtubules and the actin cytoskeleton. *Nat. Cell Biol.* **4**, 294-301.
- Krieg, M., Arboleda-Estudillo, Y., Puech, P. H., Kafer, J., Graner, F., Muller, D. J. and Heisenberg, C. P. (2008). Tensile forces govern germ-layer organization in zebrafish. *Nat. Cell Biol.* **10**, 429-436.
- Kwan, K. M. and Kirschner, M. W. (2005). A microtubule-binding Rho-GEF controls cell morphology during convergent extension of *Xenopus laevis*. *Development* **132**, 4599-4610.
- Lane, M. C. and Keller, R. (1997). Microtubule disruption reveals that Spemann's Organizer is subdivided into two domains by the vegetal alignment zone. *Development* **124**, 895-906.

- Leach, J. B., Brown, X. Q., Jacot, J. G., Dimilla, P. A. and Wong, J. Y. (2007). Neurite outgrowth and branching of PC12 cells on very soft substrates sharply decreases below a threshold of substrate rigidity. *J. Neural. Eng.* **4**, 26-34.
- Lee, J. Y. and Harland, R. M. (2007). Actomyosin contractility and microtubules drive apical constriction in *Xenopus* bottle cells. *Dev. Biol.* **311**, 40-52.
- Levental, I., Georges, P. C. and Janmey, P. A. (2007). Soft biological materials and their impact on cell function. *Soft Matter* **3**, 299-306.
- Li, B., Li, F., Puskar, K. M. and Wang, J. H. (2009). Spatial patterning of cell proliferation and differentiation depends on mechanical stress magnitude. *J. Biomech.* **42**, 1622-1627.
- Litman, P., Amieva, M. R. and Furthmayr, H. (2000). Imaging of dynamic changes of the actin cytoskeleton in microextensions of live NIH3T3 cells with a GFP fusion of the F-actin binding domain of moesin. *BMC Cell Biol.* **1**, 1.
- Machesky, L. M. and Hall, A. (1997). Role of actin polymerization and adhesion to extracellular matrix in Rac- and Rho-induced cytoskeletal reorganization. *J. Cell Biol.* **138**, 913-926.
- Nagayama, K. and Matsumoto, T. (2008). Contribution of actin filaments and microtubules to quasi-in situ tensile properties and internal force balance of cultured smooth muscle cells on a substrate. *Am. J. Physiol. Cell Physiol.* **295**, C1569-C1578.
- Nakaya, Y., Sukowati, E. W., Wu, Y. and Sheng, G. (2008). RhoA and microtubule dynamics control cell-basement membrane interaction in EMT during gastrulation. *Nat. Cell Biol.* **10**, 765-775.
- Nandadasa, S., Tao, Q., Menon, N. R., Heasman, J. and Wylie, C. (2009). N- and E-cadherins in *Xenopus* are specifically required in the neural and non-neural ectoderm, respectively, for F-actin assembly and morphogenetic movements. *Development* **136**, 1327-1338.
- Ninomiya, H. and Winklbauer, R. (2008). Epithelial coating controls mesenchymal shape change through tissue-positioning effects and reduction of surface-minimizing tension. *Nat. Cell Biol.* **10**, 61-69.
- Paszek, M. J., Zahir, N., Johnson, K. R., Lakins, J. N., Rozenberg, G. I., Gefen, A., Reinhart-King, C. A., Margulies, S. S., Dembo, M., Boettiger, D. et al. (2005). Tensional homeostasis and the malignant phenotype. *Cancer Cell* **8**, 241-254.
- Potard, U. S., Butler, J. P. and Wang, N. (1997). Cytoskeletal mechanics in confluent epithelial cells probed through integrins and E-cadherins. *Am. J. Physiol. Cell Physiol.* **272**, C1654-C1663.
- Priess, J. R. and Hirsh, D. I. (1986). *Caenorhabditis elegans* morphogenesis: the role of the cytoskeleton in elongation of the embryo. *Dev. Biol.* **117**, 156-173.
- Puech, P. H., Taubenberger, A., Ulrich, F., Krieg, M., Muller, D. J. and Heisenberg, C. P. (2005). Measuring cell adhesion forces of primary gastrulating cells from zebrafish using atomic force microscopy. *J. Cell Sci.* **118**, 4199-4206.
- Ridley, A. J. (2006). Rho GTPases and actin dynamics in membrane protrusions and vesicle trafficking. *Trends Cell. Biol.* **16**, 522-529.
- Rieu, J. P., Barentin, C., Maeda, Y. and Sawada, Y. (2005). Direct mechanical force measurements during the migration of Dictyostelium slugs using flexible substrata. *Biophys. J.* **89**, 3563-3576.
- Rotsch, C. and Radmacher, M. (2000). Drug-induced changes of cytoskeletal structure and mechanics in fibroblasts: an atomic force microscopy study. *Biophys. J.* **78**, 520-535.
- Russ, J. C. (1999). *The Image Processing Handbook*. Boca Raton, FL: CRC Press LLC.
- Ryan, X. P., Alldritt, J., Svenningson, P., Allen, P. B., Wu, G. Y., Nairn, A. C. and Greengard, P. (2005). The Rho-specific GEF Lfc interacts with neurabin and spinophilin to regulate dendritic spine morphology. *Neuron* **47**, 85-100.
- Sakamoto, T., Limouze, J., Combs, C. A., Straight, A. F. and Sellers, J. R. (2005). Blebbistatin, a myosin II inhibitor, is photoinactivated by blue light. *Biochemistry* **44**, 584-588.
- Sater, A. K., Steinhardt, R. A. and Keller, R. (1993). Induction of neuronal differentiation by planar signals in *Xenopus* embryos. *Dev. Dyn.* **197**, 268-280.
- Sato, M., Theret, D. P., Wheeler, L. T., Ohshima, N. and Nerem, R. M. (1990). Application of the micropipette technique to the measurement of cultured porcine aortic endothelial cell viscoelastic properties. *J. Biomech. Eng.* **112**, 263-268.
- Schiff, P. B., Fant, J. and Horwitz, S. B. (1979). Promotion of microtubule assembly in vitro by taxol. *Nature* **277**, 665-667.
- Schoenwolf, G. C. and Smith, J. L. (1990). Epithelial cell wedging: a fundamental cell behavior contributing to hinge point formation during epithelial morphogenesis. *Semin. Dev. Biol.* **1**, 325-334.
- Settleman, J. (2001). Rac 'n Rho: the music that shapes a developing embryo. *Dev. Cell* **1**, 321-331.
- Sivaramakrishnan, S., DeGiulio, J. V., Lorand, L., Goldman, R. D. and Ridge, K. M. (2008). Micromechanical properties of keratin intermediate filament networks. *Proc. Natl. Acad. Sci. USA* **105**, 889-894.
- Sive, H. L., Grainger, R. M. and Harland, R. M. (2000). *Early Development of Xenopus laevis: a Laboratory Manual*, pp. 338. Cold Spring Harbor, NY: Cold Spring Harbor Laboratory Press.
- Smedley, M. J. and Stanisstreet, M. (1986). Calcium and neurulation in mammalian embryos. II. Effects of cytoskeletal inhibitors and calcium antagonists on the neural folds of rat embryos. *J. Embryol. Exp. Morphol.* **93**, 167-178.
- Sokal, R. R. and Rohlf, F. J. (1994). *Biometry*. New York: W. H. Freeman and Company.
- Solnica-Krezel, L. and Driever, W. (1994). Microtubule arrays of the zebrafish yolk cell: organization and function during epiboly. *Development* **120**, 2443-2455.
- Solon, J., Levental, I., Sengupta, K., Georges, P. C. and Janmey, P. A. (2007). Fibroblast adaptation and stiffness matching to soft elastic substrates. *Biophys. J.* **93**, 4453-4461.
- Somlyo, A. P. and Somlyo, A. V. (2000). Signal transduction by G-proteins, rho-kinase and protein phosphatase to smooth muscle and non-muscle myosin II. *J. Physiol.* **522**, 177-185.
- Stamenovic, D., Liang, Z., Chen, J. and Wang, N. (2002a). Effect of the cytoskeletal prestress on the mechanical impedance of cultured airway smooth muscle cells. *J. Appl. Physiol.* **92**, 1443-1450.
- Stamenovic, D., Mijailovich, S. M., Tolic-Norrelykke, I. M., Chen, J. and Wang, N. (2002b). Cell prestress. II. Contribution of microtubules. *Am. J. Physiol. Cell Physiol.* **282**, C617-C624.
- Stern, C. D. (2004). *Gastrulation: From Cells to Embryo*. Cold Spring Harbor, NY: Cold Spring Harbor Laboratory Press.
- Straight, A. F., Cheung, A., Limouze, J., Chen, I., Westwood, N. J., Sellers, J. R. and Mitchison, T. J. (2003). Dissecting temporal and spatial control of cytokinesis with a myosin II inhibitor. *Science* **299**, 1743-1747.
- Tahinci, E. and Symes, K. (2003). Distinct functions of Rho and Rac are required for convergent extension during *Xenopus* gastrulation. *Dev. Biol.* **259**, 318-335.
- Takai, E., Costa, K. D., Shaheen, A., Hung, C. T. and Guo, X. E. (2005). Osteoblast elastic modulus measured by atomic force microscopy is substrate dependent. *Ann. Biomed. Eng.* **33**, 963-971.
- Tao, Q., Nandadasa, S., McCrea, P. D., Heasman, J. and Wylie, C. (2007). G-protein-coupled signals control cortical actin assembly by controlling cadherin expression in the early *Xenopus* embryo. *Development* **134**, 2651-2661.
- Tomasek, J. J. and Hay, E. D. (1984). Analysis of the role of microfilaments and microtubules in acquisition of bipolarity and elongation of fibroblasts in hydrated collagen gels. *J. Cell Biol.* **99**, 536-549.
- Trepat, X., Wasserman, M. R., Angelini, T. E., Millet, E., Weitz, D. A., Butler, J. P. and Fredberg, J. J. (2009). Physical forces during collective cell migration. *Nat. Phys.* **5**, 426-430.
- Trickey, W. R., Vail, T. P. and Guilak, F. (2004). The role of the cytoskeleton in the viscoelastic properties of human articular chondrocytes. *J. Orthop. Res.* **22**, 131-139.
- Trinkaus, J. P. (1984). *Cells Into Organs: the Forces That Shape the Embryo*. Englewood Cliffs: Prentice-Hall Inc.
- Tsapara, A., Luthert, P., Greenwood, J., Hill, C. S., Matter, K. and Balda, M. S. (2010). The RhoA activator GEF-H1/Lfc is a TGF- β target gene and effector that regulates α -smooth muscle actin expression and cell migration. *Mol. Biol. Cell.* **21**, 860-870.
- Valentine, M. T., Perlman, Z. E., Mitchison, T. J. and Weitz, D. A. (2005). Mechanical properties of *Xenopus* egg cytoplasmic extracts. *Biophys. J.* **88**, 680-689.
- Verin, A. D., Birukova, A., Wang, P., Liu, F., Becker, P., Birukov, K. and Garcia, J. G. (2001). Microtubule disassembly increases endothelial cell barrier dysfunction: role of MLC phosphorylation. *Am. J. Physiol. Lung Cell. Mol. Physiol.* **281**, L565-L574.
- Vincent, J. V. (1990). *Structural Biomaterials*. Princeton: Princeton University Press.
- von Dassow, M. and Davidson, L. A. (2009). Natural variation in embryo mechanics: gastrulation in *Xenopus laevis* is highly robust to variation in tissue stiffness. *Dev. Dyn.* **238**, 2-18.
- Wainwright, S. A., Biggs, W. D., Currey, J. D. and Gosline, J. M. (1976). *Mechanical Design in Organisms*. New York: John Wiley and Sons.
- Wallingford, J. B., Rowning, B. A., Vogeli, K. M., Rothbacher, U., Fraser, S. E. and Harland, R. M. (2000). Dishevelled controls cell polarity during *Xenopus* gastrulation. *Nature* **405**, 81-85.
- Wang, N. (1998). Mechanical interactions among cytoskeletal filaments. *Hypertension* **32**, 162-165.
- Wang, N., Naruse, K., Stamenovic, D., Fredberg, J. J., Mijailovich, S. M., Tolic-Norrelykke, I. M., Polte, T., Mannix, R. and Ingber, D. E. (2001). Mechanical behavior in living cells consistent with the tensegrity model. *Proc. Natl. Acad. Sci. USA* **98**, 7765-7770.
- Watanabe, N., Kato, T., Fujita, A., Ishizaki, T. and Narumiya, S. (1999). Cooperation between mDia1 and ROCK in Rho-induced actin reorganization. *Nat. Cell Biol.* **1**, 136-143.
- Wozniak, M. A. and Chen, C. S. (2009). Mechanotransduction in development: a growing role for contractility. *Nat. Rev. Mol. Cell Biol.* **10**, 34-43.
- Wu, Z. Z., Zhang, G., Long, M., Wang, H. B., Song, G. B. and Cai, S. X. (2000). Comparison of the viscoelastic properties of normal hepatocytes and hepatocellular carcinoma cells under cytoskeletal perturbation. *Biorheology* **37**, 279-290.
- Zhou, J., Kim, H. Y. and Davidson, L. A. (2009). Actomyosin stiffens the vertebrate embryo during critical stages of elongation and neural tube closure. *Development* **136**, 677-688.
- Zwaan, J. and Hendrix, R. W. (1973). Changes in cell and organ shape during early development of the ocular lens. *Am. Zool.* **13**, 1039-1049.